2019

α-Conotoxin Vc1.1 structure-activity relationship at the human α9α10 nicotinic acetylcholine receptor investigated by minimal side chain replacement

Xin Chu
Ocean University of China

Han Shen Tae
University of Wollongong, hstae@uow.edu.au

Qingliang Xu
Ocean University of China

Tao Jiang
Ocean University of China

David J. Adams
University of Wollongong, djadams@uow.edu.au

See next page for additional authors

α-Conotoxin Vc1.1 structure-activity relationship at the human α9α10 nicotinic acetylcholine receptor investigated by minimal side chain replacement

Abstract

α-Conotoxin Vc1.1 inhibits the nicotinic acetylcholine receptor (nAChR) α9α10 subtype and has the potential to treat neuropathic chronic pain. To date, the crystal structure of Vc1.1-bound α9α10 nAChR remains unavailable; thus, understanding the structure–activity relationship of Vc1.1 with the α9α10 nAChR remains challenging. In this study, the Vc1.1 side chains were minimally modified to avoid introducing large local conformation perturbation to the interactions between Vc1.1 and α9α10 nAChR. The results suggest that the hydroxyl group of Vc1.1, Y10, forms a hydrogen bond with the carbonyl group of α9 N107 and a hydrogen bond donor is required. However, Vc1.1 S4 is adjacent to the α9 D166 and D169, and a positive charge residue at this position increases the binding affinity of Vc1.1. Furthermore, the carboxyl group of Vc1.1, D11, forms two hydrogen bonds with α9 N154 and R81, respectively, whereas introducing an extra carboxyl group at this position significantly decreases the potency of Vc1.1. Second-generation mutants of Vc1.1 [S4 Dab, N9A] and [S4 Dab, N9W] increased potency at the α9α10 nAChR by 20-fold compared with that of Vc1.1. The [S4 Dab, N9W] mutational effects at positions 4 and 9 of Vc1.1 are not cumulative but are coupled with each other. Overall, our findings provide valuable insights into the structure–activity relationship of Vc1.1 with the α9α10 nAChR and will contribute to further development of more potent and specific Vc1.1 analogues.

Disciplines

Medicine and Health Sciences

Publication Details

Chu, X., Tae, H., Xu, Q., Jiang, T., Adams, D. J. & Yu, R. (2019). α-Conotoxin Vc1.1 structure-activity relationship at the human α9α10 nicotinic acetylcholine receptor investigated by minimal side chain replacement. ACS Chemical Neuroscience, 10 (10), 4328-4336.

Authors

Xin Chu, Han Shen Tae, Qingliang Xu, Tao Jiang, David J. Adams, and Rilei Yu

α-Conotoxin Vc1.1 Structure-Activity Relationship at the Human α9α10 Nicotinic Acetylcholine Receptor Investigated by Minimal Side Chain Replacement

Xin Chu,[1,2‡] Han-Shen Tae,[3‡*] Qingliang Xu,[1,2] Tao Jiang,[1,2] David J. Adams,[3] and Rilei Yu[1,2,4*]

[1]*Key Laboratory of Marine Drugs, Chinese Ministry of Education, School of Medicine and Pharmacy, Ocean University of China, 5 Yushan Road, Qingdao 266003, China*

[2] *Laboratory for Marine Drugs and Bioproducts, Qingdao National Laboratory for Marine Science and Technology, Qingdao 266003, China*

[3] *Illawarra Health and Medical Research Institute (IHMRI), University of Wollongong, Wollongong, New South Wales 2522, Australia*

[4]*Innovation Center for Marine Drug Screening & Evaluation, Qingdao National Laboratory for Marine Science and Technology, Qingdao 266003, China*

[*] Corresponding authors: hstae@uow.edu.au or ryu@ouc.edu.cn

[‡] Both authors contributed equally to this manuscript.

ABSTRACT

α-Conotoxin Vc1.1 inhibits the nicotinic acetylcholine receptor (nAChR) α9α10 subtype and has the potential to treat neuropathic chronic pain. To date, the crystal structure of Vc1.1 bound-α9α10 nAChR remains unavailable, thus understanding the structure-activity relationship of Vc1.1 with the α9α10 nAChR remains challenging. In this study, the Vc1.1 side chains were minimally modified to avoid introducing large local conformation perturbation to the interactions between Vc1.1 and α9α10 nAChR. The results suggest that the hydroxyl group of Vc1.1, Y10, forms a hydrogen bond with the carbonyl group of α9 N107 and a hydrogen bond donor is required, whereas Vc1.1 S4 is adjacent to the α9 D166 and D169, and a positive charge residue at this position increases the binding affinity of Vc1.1. Furthermore, the carboxyl group of Vc1.1, D11, forms two hydrogen bonds with α9 N154 and R81 respectively, whereas introducing an extra carboxyl group at this position significantly decreases the potency of Vc1.1. Second generation mutants of Vc1.1 [S4Dab, N9A] and [S4Dab, N9W] increased potency at the α9α10 nAChR by 20-fold compared with that of Vc1.1. The [S4Dab, N9W] mutational effects at positions 4 and 9 of Vc1.1 are not cumulative but are coupled with each other. Overall, our findings provide valuable insights into the structure-activity relationship of Vc1.1 with the α9α10 nAChR and will contribute to further development of more potent and specific Vc1.1 analogues.

KEYWORDS: α-Conotoxin, nicotinic acetylcholine receptor; structure-activity relationship; unnatural amino acids; molecular dynamics simulations; mutagenesis

1. Introduction

Conotoxins are disulfide-rich peptides from the venom of marine snails of the *Conus* genus.[1-3] The conopeptides range from 10 to 40 amino acids in length and have a compact structure stabilized by several disulfide bonds.[4] Compared with other natural peptide toxins, conotoxins have considerable advantages such as relatively small molecular mass, structural stability, high selectivity, potency, and easy synthesis.[5-9]

α-Conotoxins were one of the earliest discovered conotoxins, usually composed of 12 to 30 amino acid residues,[10] and can specifically target nicotinic acetylcholine receptors (nAChRs).[11] Several α-conotoxins have shown promising therapeutic potential[12] with a most prominent example being α-conotoxin Vc1.1 (Figure 1A).[13] Vc1.1 is a 16 amino acid, disulfide-bonded peptide identified from the venom of *C. victoria*[14] and potently inhibits the α9α10 nAChR.[15-17]

nAChRs are pentameric ligand-gated ion channels consisting of an extracellular domain, a transmembrane domain and an intracellular domain and are expressed in the central and peripheral nervous systems and non-neuronal cells.[18,19] The conotoxin binding site is located at the extracellular domain contributed by the principal (+) and complementary (−) components of two adjacent subunits (α1-α10, β1-β4, γ, δ or ε).[20] In the nervous system, they mediate the role of the neurotransmitter acetylcholine and are involved in rapid synaptic transmission.[21-23] The non-neuronal functions of nAChRs include cellular proliferation and regulation of the immune system. There are many different nAChR subtypes with preferential distribution in the nervous system,

which mediate different physiological processes.[24] There is also considerable interest in modulating nAChRs to treat nervous system disorders such as Alzheimer's disease, Parkinson's disease, schizophrenia, depression, attention deficit, hyperactivity disorder and tobacco addiction.[25-27]

The evidence that the nAChRs play a role in a number of different neuronal functions and disorders has given impetus to the search for drugs that selectively modulate different nAChR subtypes.[28] The α9 and α10 subunits form heteromeric nAChRs in the mammalian cochlea and mediate postsynaptic transmission between the olivocochlear fibres and the outer hair cells.[29-31] The α9α10 nAChR (Figure 1B) has also been implicated in chronic pain and has been proposed to be a novel target for analgesics.[32] Although the antagonism of α9α10 nAChR by α-conotoxin Vc1.1 has been speculated to be responsible for its analgesic effects, the *in vivo* target remains controversial as the G protein-coupled $GABA_B$ receptor has also been proposed as the site of action.[33,34]

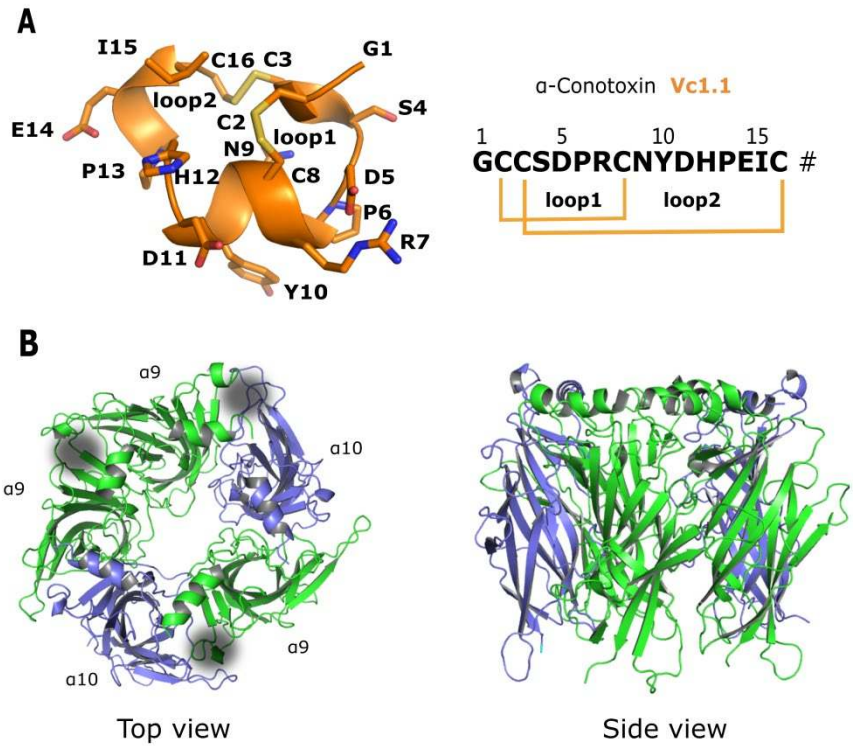

Figure 1. Structures of the α-conotoxin Vc1.1 and the extracellular domain of the α9α10 nAChR. (A) The NMR-derived distance and angle restrained (PDB code: 2H8S) structure of Vc1.1. The backbone and side chains of Vc1.1 are shown in cartoon and stick representations, respectively. α-Conotoxin Vc1.1 is a 16-amino acid peptide and has two disulfide bonds and an amidated C-terminus (represented by "#" in the sequence). (B) The extracellular ligand binding domain of the α9α10 nAChR. The α-conotoxin binding site is putatively located at the cleft between the α10(+) and α9(−) components or α9(+) and α9(−)components (grey cloud).

To date, the crystal structure of Vc1.1 bound-α9α10 nAChR remains unavailable, and computational modeling in combination with mutagenesis studies have been used as an effective method for understanding the structure-activity relationship. Previously, Yu *et al*. (2013) proposed the α10(+)-α9(−) interface as the favourable binding site of Vc1.1 at the $(\alpha9)_2(\alpha10)_3$ nAChR.[35] Additionally, residue 59 (T in rat and I in human) at the α9 subunit (−) component determined the selectivity of Vc1.1 for the rat

$(\alpha9)_2(\alpha10)_3$ nAChR compared to the human (h) $(\alpha9)_2(\alpha10)_3$ nAChR. Subsequently, Indurthi *et al*. (2014) proposed that the α9(+)-α9(−) binding site in $(\alpha9)_3(\alpha10)_2$ arrangement was the most sensitive binding site for Vc1.1 rather than the α10(+)-α9(−) site.[36] Yu *et al*. (2018) performed a comprehensive computational modeling based on the proposed high and low Vc1.1 sensitivity binding sites in the $(\alpha9)_2(\alpha10)_3$ and $(\alpha9)_3(\alpha10)_2$ stoichiometries and concluded that the $(\alpha9)_3(\alpha10)_2$ arrangement uniquely contained an α9(+)-α9(−) interface binding site in which N154 at the α9(+) component formed a hydrogen bond with D11 of Vc1.1 that is responsible for the higher sensitivity of the receptor to Vc1.1.[37,38]

Despite the advancement in studying the binding mode of Vc1.1 at α9α10 nAChR based on computational modeling, understanding the structure-activity relationship of Vc1.1 with the α9α10 nAChR is hampered by the lack of high resolution crystal structures and high degree of confidence computational models of α9α10 nAChR bound to Vc1.1.

Alanine scanning data has been extensively used for validation of the computationally determined binding modes of the α-conotoxins. However, substituting long side-chained residues with alanine not only removes the functional groups, but also significantly reduces the size of the original residues which is often accompanied by a significant local conformation change in the binding interface, masking the effects of the mutation. In this study, we used molecular dynamics simulations to probe the interactions of Vc1.1 analogues with the hα9α10 nAChR binding site in order to identify the residues involved. Furthermore, we determined the

activity of systematically generated unnatural amino acid (Figure S1) analogues of Vc1.1 at heterologously expressed hα9α10 nAChR in *Xenopus* oocytes using two-electrode voltage clamp electrophysiology.

2. Results and discussion

In this study, specific Vc1.1 side chains were minimally modified to validate the previously determined binding modes of Vc1.1 and to understand the structure-activity relationship of Vc1.1 with the α9α10 nAChR.

We were interested in Vc1.1 residues 4, 6, 10 and 11 as they either form hydrogen bond or salt bridges with nearby residues of the α subunits (Figure 2A). Results from a previous alanine scanning study suggested that removal of the hydroxyl group of S4 and the carboxyl group of D11 significantly contribute to the binding affinity of Vc1.1, whereas removal of the side-chain of Y10 slightly improves the binding affinity of the Vc1.1 mutant.[39]

Results from alanine scanning support our established model in which Vc1.1 S4 forms hydrogen bond with α9 D166 (Figure 2B) and Vc1.1 D11 forms hydrogen bonds/salt-bridges with α9 residues R81 and N154 (Figure 2E). However, the results disagree with our modeling studies in which two hydrogen bonds were identified between the hydroxyl group of Vc1.1 Y10 and the backbone H atom of α9 D119 and O atom of α9 N107 (Figure 2D). Thus, the alanine scanning data cannot accurately and comprehensively explain the contribution of the side chains to the binding affinity of the α-conotoxins due to its dual effects on both the functional group and local

conformation change at the binding interface. Consequently, for more explicit and accurate understanding on the contribution of the residues in the binding of α-conotoxins to the nAChRs, mutating the peptide using amino acid residues with similar side chains is necessary.

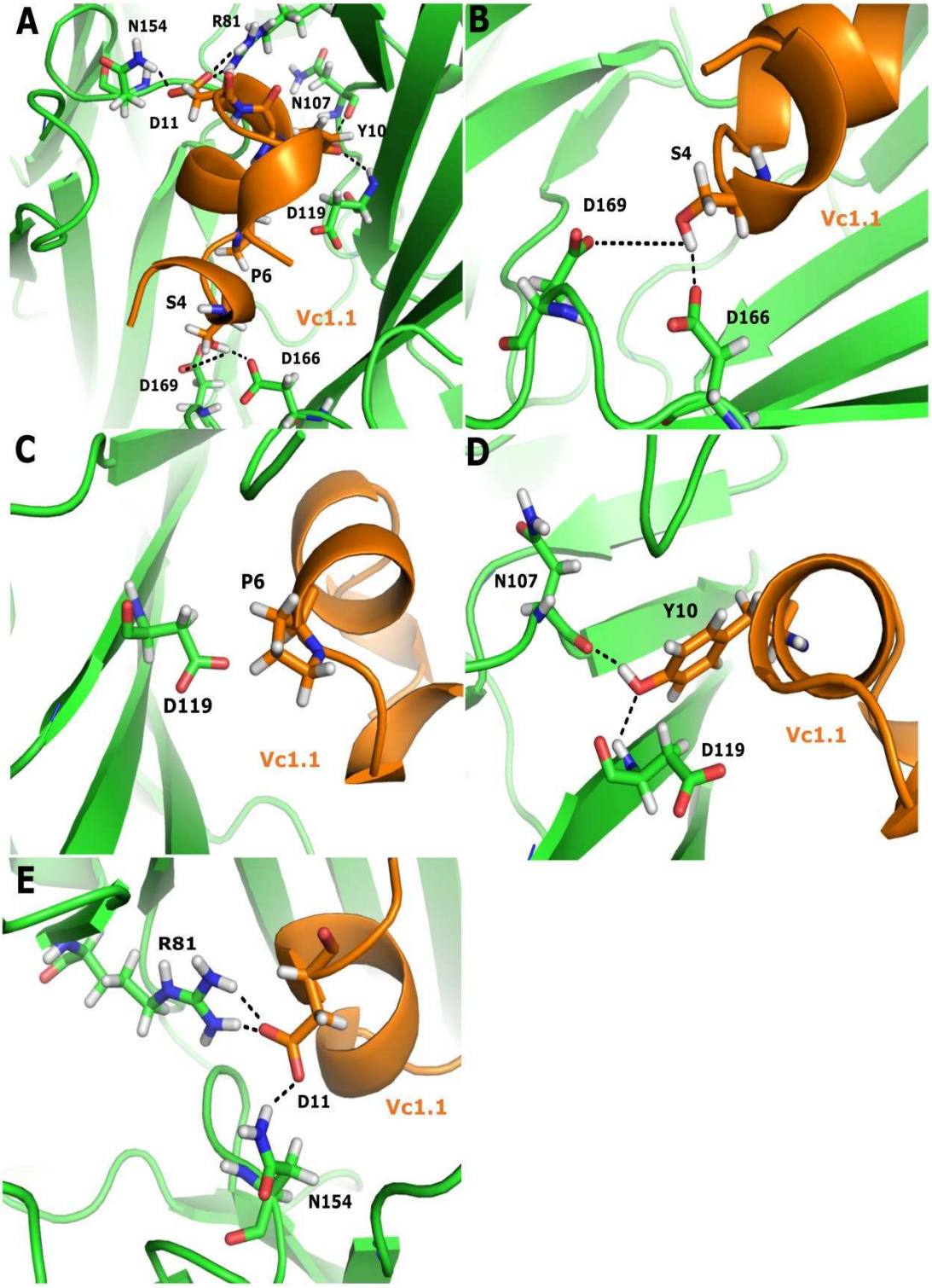

Figure 2. Binding of (A) α-conotoxin Vc1.1 (orange) at the α9(+)-α9(−) interfaces of the human α9α10 nAChR, with the binding sites of positions 4 (B), 6 (C), 10 (D) and 11 (E) magnified. Only the side chains of selected residues on the subunit of the α9(+)-α9(−) binding sites are shown. Hydrogen bonds are shown as yellow dashed

lines.

In our previous model, Vc1.1 S4 was positioned nearby α9 D169 and D166, forming a hydrogen bond with D166, and introduction of a positively charged residue at position 4 was expected to strengthen the binding affinity of the Vc1.1 mutant.[32] Thus, the side chain hydroxyl group of S4 was replaced with amine to increase its electrostatic interaction with D169 and D166. Additionally, [S4K] and [S4Dab] mutants of Vc1.1 were synthesized (Table 1, Figure S1) to investigate the influence of side chain length on the activity. Residue P6 of Vc1.1 is located in the inner part of the binding site and is close to α9 D119 (Figure 2C), therefore, introducing a hydroxyl group to P6 could potentially increase or at least maintain its activity by forming a hydrogen bond with D119.

Furthermore, we found that two hydrogen bonds were formed between the hydroxyl group of Vc1.1 Y10 and α9 residues N107 and D119 in the molecular dynamics (MD) simulation. In order to validate the contribution of the hydroxyl group to the binding affinity of Vc1.1, phenylalanine was introduced to position 10 of Vc1.1. Besides, the hydroxyl group of Y10 in Vc1.1 was replaced with F (fluoride) or Cl (chloride) (Table 1) to explore the possibility of hydrogen or halogen bond formation with nearby residues due to the removal of the hydroxyl group. Furthermore, in our previously built model,[25] D11 in Vc1.1 forms hydrogen bond/salt-bridge interactions with the side chains of α9 N154 and R81. Here, we explore the influence of the length and charge of the side chain to the potency of the peptide by replacing D11 with glutamic acid or γ-carboxyglutamic acid (Table 1, Figure S1).

TABLE 1. The peptide sequence of Vc1.1 analogues and their corresponding serial number.

Number	Peptide	Sequence
CX-1	[S4K]Vc1.1	GCCKDPRCNYDHPEIC*
CX-2	[S4Dab]Vc1.1	GCC(Dab)DPRCNYDHPEIC*
CX-3	[S4Dap]Vc1.1	GCC(Dap)DPRCNYDHPEIC*
CX-4	[P6Hyp]Vc1.1	GCCSD(Hyp)RCNYDHPEIC*
CX-5	[Y10F]Vc1.1	GCCSDPRCNFDHPEIC*
CX-6	[Y10F(4-F)]Vc1.1	GCCSDPRCN[Phe(4-F)]DHPEIC*
CX-7	[Y10F(4-Cl)]Vc1.1	GCCSDPRCN[Phe(4-Cl)]DHPEIC*
CX-8	[D11E]Vc1.1	GCCSDPRCNYEHPEIC*
CX-9	[D11(γ-E)]Vc1.1	GCCSDPRCNY(γ-E)HPEIC*

∗ represents amidation of the C-terminus.
Dab = diaminobutyric acid
Dap = diaminopropionic acid
γ-E = γ-carboxyglutamic acid
Hyp = hydroxyproline

The relative inhibitory activity of the designed Vc1.1 analogues was determined at the hα9α10 nAChRs heterologously expressed in *Xenopus* oocytes using the two-electrode voltage clamp technique. The potency of [S4Dab]Vc1.1 (CX-2) was significantly increased compared to wild-type Vc1.1, whereas the inhibitory activity of [S4Dap] (CX-3) only marginally increased (Figure 3). In contrast, the potency of [S4K]Vc1.1 (CX-1) was slightly reduced compared to Vc1.1. The K, Dab and Dap residues all possess a positively charged amine group at the side chain terminus, whereas their potency is remarkably different suggesting that appropriate length of the side chain is essential for the formation of favourable electrostatic interaction with the proposed D169 and D166 in our model (Figure 2).

The inhibitory activity of [P6Hyp]Vc1.1 (CX-4) at hα9α10 nAChRs was comparable with that of Vc1.1 (Figure 3). Thus, introducing a hydroxyl group to P6 of Vc1.1 introduced only minor effects to the activity of Vc1.1. In contrast to the comparable activity of [Y10A]Vc1.1 mutant,[39] mutation of Y10 to F10 (CX-5, 6 and 7) (Table 1) significantly reduced the inhibition of ACh-evoked currents ($p < 0.0001$) (Figure 3). Results from the [Y10F] mutation suggest that the hydroxyl group is required for the potency of Vc1.1. Additionally, both [D11E]Vc1.1 (CX-8) and [D11(γ-E)]Vc1.1 (CX-9) exhibited significantly lower potency ($p < 0.0001$) than wild-type Vc1.1 at hα9α10 nAChRs, suggesting that increasing the length of the side chain and/or the number of the negative charges substantially decreased the potency of the mutants. The change in activity of the mutants is considered to originate from the side chain replacement rather than from peptide secondary structure perturbation in consideration of their similar CD spectra absorption (Figure S2).

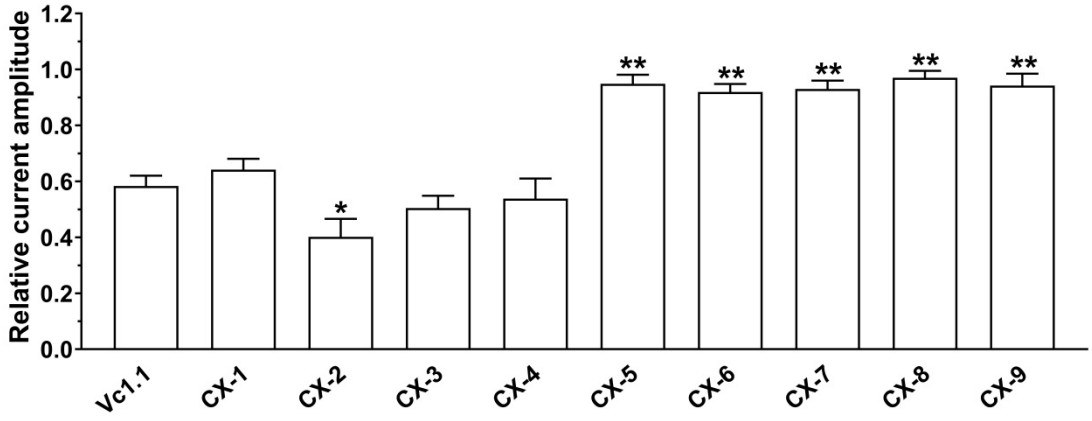

Figure 3. Bar graph of inhibition of ACh-evoked peak current amplitude mediated by hα9α10 nAChRs by 1 μM Vc1.1 and analogues (CX-1– CX-9). Whole-cell currents at hα9α10 nAChR were activated by 6 μM ACh (mean ± SEM, n = 4-12). *$p < 0.05$ and

** $p < 0.0001$, Student's t-test.

Molecular dynamics simulation of the designed Vc1.1 analogues binding to the α9α10 nAChR was performed for in-depth understanding of their interactions (Figure 4, Figure S3). Analysis of the interactions between [S4Dab]Vc1.1 and hα9α10 nAChR showed that the side chains of Dab4 formed several salt-bridges with D166, D169 and S168 of the receptor (Figure 4A, Figure S4A–C), which are responsible for the enhanced potency of [S4Dab]Vc1.1 at the hα9α10 nAChR. On the other hand, the enhanced activity of [S4Dap]Vc1.1 was contributed by hydrogen bonds formed between Dap4 with D166, D199 and T32 (Figure 4B, Figure S4D–F).

In contrast, lysine replacement of S4 interrupted the salt-bridge interactions between the amine group of lysine and D166 and D169 due to the longer side chain (Figure 4C, Figure S4G), resulting in the substantially reduced [S4K]Vc1.1 potency at hα9α10. The hydroxyl group introduced by Hyp substitution of P6 formed a hydrogen bond with the side chain of α9 D119 at the binding site (Figure 4D, Figure S4H). The hydrogen bond may compensate to some extent the hydrophobicity loss due to introducing the hydroxyl group thus, the comparable potency of Vc1.1 and [P6Hyp]Vc1.1. MD simulations of [Y10F]Vc1.1, [Y10F(4-F)]Vc1.1 or [Y10F(4-Cl)]Vc1.1 bound to the hα9α10 nAChR (Figure 4 E, F and G, respectively), suggested that neither hydrogen nor halogen bonds were formed to compensate the removal of the hydroxyl group at the tyrosine side chain. This resulted in the dramatic decreased the potency of these aforementioned Y10 mutants of Vc1.1.

The model of [D11E]Vc1.1 interaction with the hα9α10 nAChR, suggested that despite the formation of hydrogen bond between Vc1.1 E11 and α9 N154 E11 (Figure 4H, Figure S4I), the salt-bridge between E11 and α9 R81 was disrupted probably due to the highly flexible and longer side chain of E11 (Figure 4H, Figure S4J). Consequently, [D11E]Vc1.1 showed substantially decreased potency in comparison to Vc1.1. Similarly for D11γE mutant, only one of the carboxyl group formed hydrogen bond with N154 and Q157, whereas the other formed no interactions with the residues of the receptor (Figure 4I, Figure S4K,L), resulting in significantly decreased binding affinity to the hα9α10 nAChR.

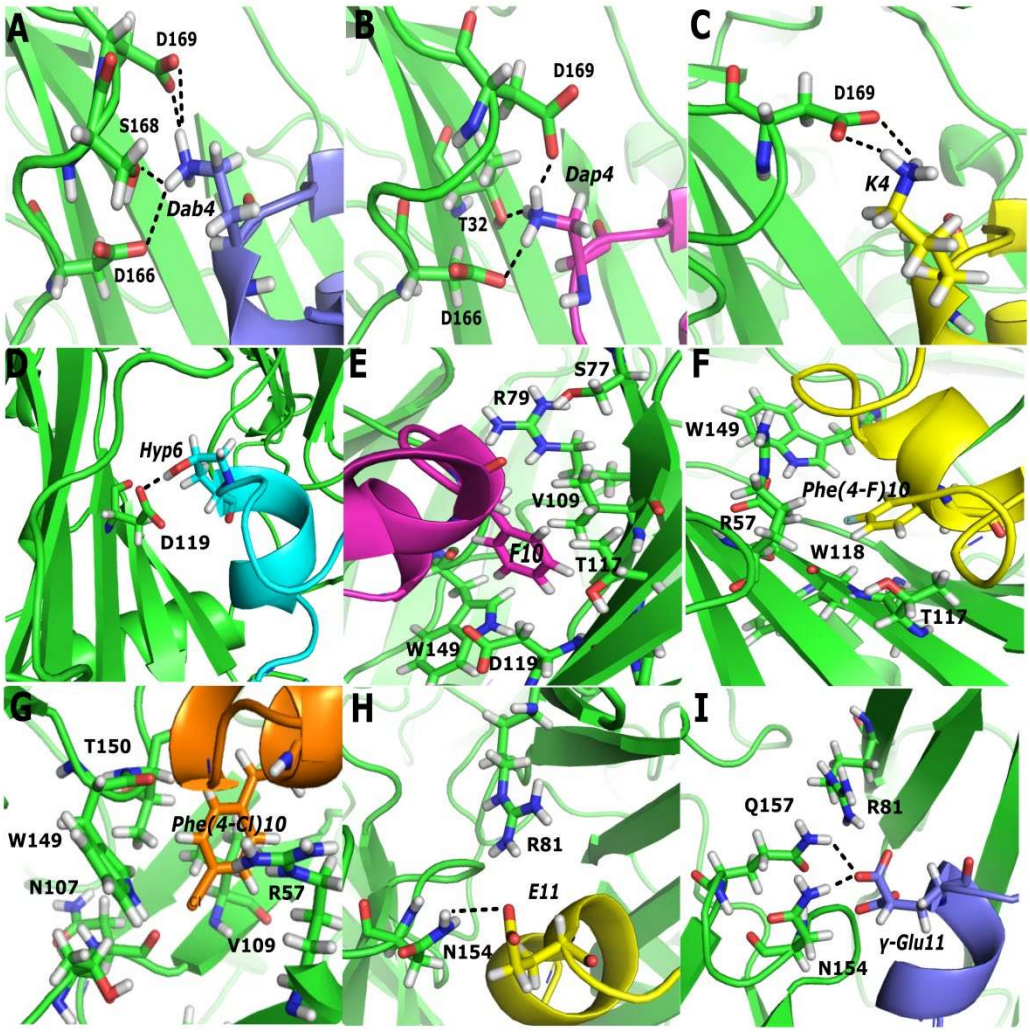

Figure 4. Interactions established by position 4, 6, 10 and 11 of Vc1.1 analogues in α9(+)-α9(−) interfaces of the hα9α10 nAChR, respectively. (A, B, C, D, E, F, G, H, I): [S4Dab]Vc1.1, [S4Dap]Vc1.1, [S4K]Vc1.1, [P6Hyp]Vc1.1, [Y10F]Vc1.1, [Y10F(4-F)]Vc1.1, [Y10F(4-Cl)]Vc1.1, [D11E]Vc1.1 and [D11(γ-E)]Vc1.1 bound to the interfaces of α9(+)-α9(−), respectively. The α9 subunits are shown in green. Vc1.1 residues are labeled in italic. The models of Vc1.1 analogues and α9α10 nAChR complexes were built based on that of Vc1.1/α9α10 nAChR complex using homology modeling and were refined using MD simulations in water explicitly.

The design of double or triple mutants by combining single mutations with enhanced activity is an effective strategy to significantly improve the potency of

conotoxins. However, in some cases residues in different positions are coupled with each other, and their mutational effects are not cumulative. Although Halai *et al*. (2009) designed the [S4K, N9A]Vc1.1 double mutant with increased potency of ~29 fold compared to Vc1.1, at the hα9/rat α10 nAChR hybrid, however, the potency of the double mutant is comparable to the single mutant [N9A]Vc1.1.[39]

Mutation of S4 to lysine led to substantial structure change in the side chain and binding orientation to accommodate the local conformation change at 4 position of Vc1.1. Similarly, the [N9A] mutation might also result in significant change in the binding orientation to the receptor. Consequently, the mutational effects of the [S4K, N9A] double mutation were not cumulative of the single mutations, since the double mutant could only select either the orientation of [S4K]Vc1.1 or [N9A]Vc1.1 upon binding to the receptor. Hence, to reduce the conformational effects introduced by the residue at position 4 of Vc1.1, residues with minimal conformational change are preferred. Compared to lysine, Dab has a shorter side chain and [S4Dab] substitution is expected to have minimal conformational impact on the binding mode of the mutant. Given the higher potency of [S4Dab]Vc1.1 than [S4Dap]Vc1.1, the [S4Dab] mutation was included in the design of Vc1.1 double mutants. In consideration of the higher potency of [N9A]Vc1.1 (CX-10) and [N9W]Vc1.1 (CX-11) (Table 2), we designed [S4Dab, N9A]Vc1.1 (CX-12) and [S4Dab, N9W]Vc1.1 (CX-13) (Table 2) as the second generation analogues of Vc1.1.

TABLE 2. The peptide sequence of the second round design of Vc1.1 analogues and their corresponding serial number.

Number	Peptide	Sequence
CX-10	[N9A]Vc1.1	GCCSDPRCAYDHPEIC*
CX-11	[N9W]Vc1.1	GCCSDPRCWYDHPEIC*
CX-12	[S4Dab, N9A]Vc1.1	GCC(Dab)DPRCAYDHPEIC*
CX-13	[S4Dab, N9W]Vc1.1	GCC(Dab)DPRCWYDHPEIC*

The second generation [S4Dab, N9A]Vc1.1 and [S4Dab, N9W]Vc1.1 analogues were chemically synthesized, and their activity was determined at heterologously expressed hα9α10 nAChR. The concentration dependent activity of both analogues was determined giving a half-maximal inhibitory concentration (IC_{50}) of 52.5 ± 3.2 nM for [S4Dab, N9A]Vc1.1 (Figure 5A), whereas the potency of [S4Dab, N9W]Vc1.1 was higher, with an IC_{50} of 38.7 ± 2.8 nM ($n \geq 5$) (Figure 5B). The analogues exhibited a 20-fold increase of potency at the hα9α10 nAChR compared to Vc1.1 (1 μM).[25] The IC_{50} of [N9A]Vc1.1 and [N9W]Vc1.1 were 185.8 ± 20.7 nM and 49.1 ± 5.0 nM ($n \geq 5$), respectively, (Figure 5A,B). The mutational effects for the [S4Dab, N9A] mutations were cumulative to some extent, whereas for [S4Dab, N9W] they are not cumulative. The [N9W] mutation can cause larger local conformational change than [N9A] mutation at the binding interface, which might counteract the favorable effects introduced by the [S4Dab] mutation for the [S4Dab, N9W]Vc1.1 double mutant.

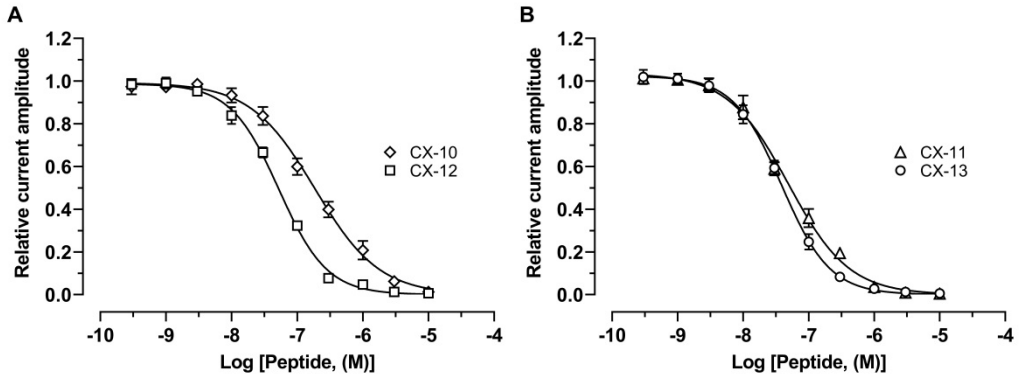

Figure 5. Concentration-response relationships of relative ACh-evoked current amplitude mediated by hα9α10 nAChR in the presence of Vc1.1 analogues (300 pM – 10 μM) A) CX-10 and CX-12 giving IC_{50}'s of 185.8 ± 20.7 nM and 52.5 ± 3.2 nM, respectively, and B) CX-11 and CX-13 giving IC_{50}'s of 49.1 ± 5.0 nM and 38.7 ± 2.8 nM (mean ± SEM, n = 5-9), respectively. Whole-cell currents at hα9α10 nAChR were activated by 6 μM ACh.

3. Conclusions

In summary, using previously built α9α10 nAChR model as guidance, we designed a library of Vc1.1 analogues by introducing residues with similar physicochemical properties to the wild-type residues in order to validate the accuracy of the model and investigated the structure-activity relationship of Vc1.1 with the hα9α10 nAChR at the atomic level. Our findings suggest that Vc1.1 S4 forms hydrogen bonds with α9 D166 and D169, and introducing positively charged residues at this position can improve the potency. The P6 is nearby D119, and the introduced Hyp6 approaches D119 and forms a hydrogen bond. In addition, the hydroxyl group at Y10 side chain forms several hydrogen bonds with residues at the (+) component of the α9 subunit. The side chain length and the number of negative charges are essential for residue at

10 position of Vc1.1. Finally, two highly potent analogues, [S4Dab, N9A]Vc1.1 and [S4Dab, N9W]Vc1.1, were designed with ~ 20-fold increased potency at the hα9α10 nAChR. Overall, our study provides valuable insights into the structure-activity relationship of Vc1.1 with the hα9α10 nAChR and will contribute to the further development of Vc1.1 analogues as molecular probes or drugs.

4. Methods and materials

4.1. Molecular dynamics simulations

All molecular dynamics (MD) simulations were performed using the AMBER 16 package with the ff14SB force field.[40, 41] Parameters for the unnatural amino acids were prepared in the Antechamber module of AMBER16. Atom partial charges for PCA (pyroglutamic acid) were produced using the R.E.D Tools.[42] The protonation states of histidine, aspartic acid and glutamic acid at the conotoxin/nAChR complexes were predicted using the PropKa 3.1 method.[43] The receptor complexes were solvated in a truncated octahedral TIP3P water box containing ~10800 water molecules. Sodium ions were added to neutralize the systems. The systems were first minimized with 3,000 steps of steepest descent and then 3,000 steps of conjugate gradient with the solute restrained to their position by a harmonic force of 100kcal $mol^{-1}\cdot Å^{-2}$. A second minimization was then performed but with all position restraints withdrawn. The systems were then gradually heated up from 50 to 300 K in the NVT ensemble over 100 ps with the solute restrained to their position using a 5 kcal $mol^{-1}\cdot Å^{-2}$ harmonic force potential. MD simulations were then carried out in the NPT ensemble, and the position restraints were gradually removed over 100 ps. The production runs

were conducted over 50 ns simulation time with pressure coupling set at 1atm and a constant temperature of 300 K. The MD simulations used a time step of 2 fs and, all bonds involving hydrogen atoms were maintained to their standard length using the SHAKE algorithm.[44] The particle-mesh Ewald (PME) method was used to model long-range electrostatic interactions.[45] MD trajectories were analyzed using VMD (http://www.ks.uiuc.edu/) and molecules were drawn using PyMol (Schrödinger, LLC).

4.2. Peptide synthesis

Briefly, Vc1.1 analogs were assembled on rink amide methylbenzhydrylamine resin (Novabiochem) using solid-phase peptide synthesis with a neutralization/2-(1H-benzotriazol-1-yl)-1,1,3,3-tetramethyluronium hexafluorophosphate activation procedure for Fmoc (N-(9-fluorenyl)methoxycarbonyl) chemistry. Cleavage was achieved by treatment with 88:5:5:2 ratio of trifluoroacetic acid (TFA), phenol, water and triisopropylsilane as scavengers, at room temperature (20−25 °C) for 3 h. TFA was evaporated at low pressure in a rotary evaporator. Peptides were precipitated with ice-cold ether, filtered, dissolved in 50% buffer A/B (buffer A consists of 90% H_2O/10% CH_3CN/0.05% TFA and buffer B consists of 90% CH_3CN/10% H_2O/0.05% TFA), and lyophilized. Crude peptides were purified by RP-HPLC on a Phenomenex C18 column, and its molecular mass was confirmed using electrospray mass spectrometry. The four cystines in the peptides were selectively oxidized in two steps. In the first step the non-protected cystines were oxidized in 0.1M NH_4HCO_3 (pH 8–8.5) at a concentration of 0.5 mg/ml, and stirred at

room temperature for 48 hours. In the second step, the Acm-protected cystine is oxidized by dissolving the peptide in an iodine/acetonitrile solution having a concentration of 5 mg/ml, and the reaction is stirred in a closed environment at 28 °C for about 2 h. Until the mass spectrometry confirms the reaction was successful, ascorbic acid was then added to stop the oxidizing reaction and the solution was stirred again until no colour was visible. After two rounds of oxidation, peptides were purified by RP-HPLC and their mass and purity were validated using electrospray-mass spectrometry (MS) and analytical RP-HPLC, respectively (Figure S5).

4.3. Electrophysiology.

RNA preparation, oocyte preparation, and expression of human α9α10 nAChRs in *Xenopus laevis* oocytes were performed as described previously.[25] Briefly, plasmids with cDNA encoding the hα9 and hα10 subunits subcloned into the oocyte expression vector pT7TS were used for mRNA preparation using the mMESSAGE mMACHINE kit (AMBION, Foster City, CA, USA). Oocytes were injected with 35 ng of mRNA for α9 and α10 subunits and then kept at 18 °C in ND96 buffer (96 mM NaCl, 2 mM KCl, 1 mM $CaCl_2$, 1 mM $MgCl_2$, and 5 mM HEPES, at pH 7.4) supplemented with 0.5 mg/L gentamicin, and 100 U/mL penicillin-streptomycin 2−7 days before recording. All procedures were approved by the University of Wollongong and University of Sydney Animal Ethics Committees.

Membrane currents were recorded at room temperature (21−23 °C) from *Xenopus* oocytes using a two-electrode (virtual ground circuit) voltage clamp with a

GeneClamp 500B amplifier and pClamp9 software interface (Molecular Devices, Sunnyvale, CA) at a holding potential –80 mV. Both the voltage-recording and current-injecting electrodes were pulled from borosilicate glass (GC150T-15, Harvard Apparatus, Holliston, MA, USA) and had resistances of 0.3−1.0 MΩ when filled with 3 M KCl.

Oocytes expressing were incubated with 100 μM BAPTA-AM at 18 ºC for ~3 h before recording and perfused with ND115 solution containing (in mM): 115 NaCl, 2.5 KCl, 1.8 $CaCl_2$, 10 HEPES, pH 7.4 at a rate of 2 mL/min. Initially, oocytes were briefly washed with ND115 followed by 3 applications of ACh at a half-maximal effective concentration for hα9α10 nAChR (EC_{50} = 6 μM)[25] and 3 min washouts between ACh applications followed with 5 min incubation times for the peptide. Peak current amplitudes before (I_{ACh}) and after ($I_{ACh+peptide}$) incubation were measured using Clampfit 10.7 software (Molecular Devices, Sunnyvale, CA, USA) and the relative current amplitude, $I_{ACh+peptide}/I_{ACh}$ was used to assess the activity of the peptides at hα9α10 nAChR.

4.4. Data analysis

Concentration-response relationships for the peptides were determined using the Hill equation (GraphPad Prism 7 Software, La Jolla, CA, USA). The calculated IC_{50} (half-maximal inhibitory concentration) values were reported with error of the fit. The electrophysiological results were compared using unpaired Student's t-test. Values of $P \leq 0.05$ were considered statistically significant.

Acknowledgements

This work was supported by the grant from the Fundamental Research Funds for the Central Universities (201762011 and 201941012), the National Laboratory Director Fund (QNLM201709), and the Marine S&T Fund of Shandong Province for Pilot National Laboratory for Marine Science and Technology (Qingdao) (No. 2018SDKJ0402), and an Australian Research Council (ARC) Discovery Project Grant (DP150103990 awarded to D.J.A.).

References：

(1) Olivera, B. M., Gray, W. R., Zeikus, R., McIntosh, J. M., Varga, J., Rivier, J., de Santos, V., and Cruz, L. J. (1985) Peptide neurotoxins from fish-hunting cone snails. *Science (N.Y.) 230*, 1338-1343.

(2) Olivera, B. M., Rivier, J., Clark, C., Ramilo, C. A., Corpuz, G. P., Abogadie, F. C., Mena, E. E., Woodward, S. R., Hillyard, D. R., and Cruz, L. J. (1990) Diversity of *Conus* neuropeptides. *Science (N.Y.) 249*, 257-263.

(3) Terlau, H., and Olivera, B. M. (2004) *Conus* venoms: A rich source of novel ion channel-targeted peptides. *Physiol. Rev. 84*, 41-68.

(4) Akondi, K. B., Muttenthaler, M., Dutertre, S., Kaas, Q., Craik, D. J., Lewis, R. J., and Alewood, P. F. (2014) Discovery, synthesis, and structure activity relationships of conotoxins. *Chem. Rev. 114*, 5815-5847.

(5) Altier, C., Dale, C. S., Kisilevsky, A. E., Chapman, K., Castiglioni, A. J., Matthews, E. A., Evans, R. M., Dickenson, A. H., Lipscombe, D., Vergnolle, N., and Zamponi, G. W. (2007) Differential role of N-type calcium channel splice isoforms in pain. *J. Neurosci. 27*, 6363-6373.

(6) Halai, R., and Craik, D. J. (2009) Conotoxins: natural product drug leads. *Nat. Prod. Rep. 26*, 526-536.

(7) Lewis, R. J., Dutertre, S., Vetter, I., and Christie, M. J. (2012) *Conus* venom peptide pharmacology, *Pharmacol. Rev. 64*, 259-298.

(8) Lewis, R. J., Nielsen, K. J., Craik, D. J., Loughnan, M. L., Adams, D. A., Sharpe, I. A., Luchian, T., Adams, D. J., Bond, T., Thomas, L., Jones, A., Matheson, J. L., Drinkwater, R., Andrews, P. R., and Alewood, P. F. (2000) Novel omega-conotoxins from *Conus catus* discriminate among neuronal calcium channel subtypes, *J. Biol. Chem. 275*, 35335-35344.

(9) Millar, N. S., and Gotti, C. (2009) Diversity of vertebrate nicotinic acetylcholine receptors. *Neuropharmacology 56*, 237-246.

(10) Olivera, B. M. (1997) EE Just lecture, 1996 - *Conus* venom peptides, receptor and ion channel targets, and drug design: 50 million years of neuropharmacology. *Mol. Biol.Cell 8*, 2101-2109.

(11) Livett, B. G., Gayler, K. R., and Khalil, Z. (2004) Drugs from the sea: Conopeptides as potential therapeutics. *Curr. Med. Chem. 11*, 1715-1723.

(12) Dutertre, S., and Lewis, R. J. (2010) Use of venom peptides to probe ion channel structure and function. *J. Biol. Chem. 285*, 13315-13320.

(13) Clark, R. J., Jensen, J., Nevin, S. T., Callaghan, B. P., Adams, D. J., and Craik, D. J. (2010) The engineering of an orally active conotoxin for the treatment of neuropathic pain. *Angewandte Chemie-Intl. Ed. 49*, 6545-6548.

(14) Sandall, D. W., Satkunanathan, N., Keays, D. A., Polidano, M. A., Liping, X., Pham, V., Down, J. G., Khalil, Z., Livett, B. G., and Gayler, K. R. (2003) A novel α-conotoxin identified by gene sequencing is active in suppressing the vascular response to selective stimulation of sensory nerves in vivo. *Biochemistry 42*, 6904-6911.

(15) Carstens, B. B., Clark, R. J., Daly, N. L., Harvey, P. J., Kaas, Q., and Craik, D. J. (2011) Engineering of conotoxins for the treatment of pain. *Curr. Pharmac. Design 17*, 4242-4253.

(16) Livett, B. G., Sandall, D. W., Keays, D., Down, J., Gayler, K. R., Satkunanathan, N., and

Khalil, Z. (2006) Therapeutic applications of conotoxins that target the neuronal nicotinic acetylcholine receptor. *Toxicon 48*, 810-829.
(17) Satkunanathan, N., Livett, B., Gayler, K., Sandall, D., Down, J., and Khalil, Z. (2005) Alpha-conotoxin Vc1.1 alleviates neuropathic pain and accelerates functional recovery of injured neurones. *Brain Res. 1059*, 149-158.
(18) Albuquerque, E.X., Pereira, E.F., Alkondon, M., and Rogers, S.W. (2009) Mammalian nicotinic acetylcholine receptors: from structure to function. *Physiol Rev*. *89*(1), 73-120.
(19) Zoli, M, Pucci, S, Vilella, A, and Gotti, C. (2018) Neuronal and Extraneuronal Nicotinic Acetylcholine Receptors. *Curr Neuropharmacol*. *16*(4), 338-349.
(20) Dutertre, S., and Lewis, R.J. (2004) Computational approaches to understand α-conotoxin interactions at neuronal nicotinic receptors. *Eur J Biochem*. *271*(12), 2327-2334.
(21) Dani, J. A., and Bertrand, D. (2007) Nicotinic acetylcholine receptors and nicotinic cholinergic mechanisms of the central nervous system. *Ann Rev Pharmacol Toxicol 47*, 699-729.
(22) Hurst, R., Rollema, H., and Bertrand, D. (2013) Nicotinic acetylcholine receptors: from basic science to therapeutics. *Pharmacology & Therapeutics 137*(1), 22-54.
(23) Elgoyhen, A.B., and Katz, E. (2012) The efferent medial olivocochlear-hair cell synapse. *J. Physiol. (Paris)* 106(1-2), 47-56
(24) Zoli, M., Pistillo, F., and Gotti, C. (2015) Diversity of native nicotinic receptor subtypes in mammalian brain, *Neuropharmacology 96*, 302-311.
(25) Levin, E. D., and Rezvani, A. H. (2007) Nicotinic interactions with antipsychotic drugs, models of schizophrenia and impacts on cognitive function, *Biochem. Pharmacol. 74*, 1182-1191.
(26) Kutlu, M. G., and Gould, T. J. (2015) Nicotinic receptors, memory, and hippocampus. *Current Topics in Behavioral Neurosciences 23*, 137-163.
(27) Dineley, K. T., Pandya, A. A., and Yakel, J .L. (2015) Nicotinic ACh receptors as therapeutic targets in CNS disorders. *Trends in Pharmacological Sciences* 36(2), 96-108.
(28) Elgoyhen, A. B., Katz, E., and Fuchs, P. A. (2009) The nicotinic receptor of cochlear hair cells: A possible pharmacotherapeutic target? *Biochem. Pharmacol. 78*, 712-719.
(29) Elgoyhen, A. B., Vetter, D. E., Katz, E., Rothlin, C. V., Heinemann, S. F., and Boulter, J. (2001) α10: A determinant of nicotinic cholinergic receptor function in mammalian vestibular and cochlear mechanosensory hair cells. *Proc. Natl. Acad. Sci., U.S.A. 98*, 3501-3506.
(30) Sgard, F., Charpantier, E., Bertrand, S., Walker, N., Caput, D., Graham, D., Bertrand, D., and Besnard, F. (2002) A novel human nicotinic receptor subunit, α10, that confers functionality to the α9-subunit. *Mol. Pharmacol. 61*, 150-159.
(31) Gómez-Casati, M.E., Fuchs, P.A., Elgoyhen, A.B., and Katz, E. (2005) Biophysical and pharmacological characterization of nicotinic cholinergic receptors in rat cochlear inner hair cells. *J. Physiol. 566*(Pt 1), 103-118
(32) Mohammadi, S. A., and Christie, M. J. (2015) Conotoxin interactions with α9α10-nAChRs: Is the α9α10-nicotinic acetylcholine receptor an important therapeutic target for pain management? *Toxins 7*, 3916-3932.
(33) Sadeghi, M., McArthur, J.R., Finol-Urdaneta, R.K. and Adams, D.J. (2017) Analgesic conopeptides targeting G protein-coupled receptors reduce excitability of sensory neurons. *Neuropharmacology 127*, 116-123.

(34) Sadeghi, M., Carstens, B.B., Callaghan, B.P., Daniel, J.T., Tae, H-S., O'Donnell, T., Castro, J., Brierley, S.M., Adams, D.J., Craik, D.J. and Clark, R.J. (2018) Structure-activity studies reveal the molecular basis for $GABA_B$ receptor-mediated inhibition of high voltage-activated calcium channels by α-conotoxin Vc1.1. *ACS Chem. Biol. 13*(6), 1577-1587.
(35) Yu, R., Kompella, S. N., Adams, D. J., Craik, D. J., and Kaas, Q. (2013) Determination of the α-conotoxin Vc1.1 binding site on the α9α10 nicotinic acetylcholine receptor. *J..Med. Chem. 56*, 3557-3567.
(36)Indurthi, D. C., Pera, E., Kim, H.-L., Chu, C., McLeod, M. D., McIntosh, J. M., Absalom, N. L., and Chebib, M. (2014) Presence of multiple binding sites on α9α10 nAChR receptors alludes to stoichiometric-dependent action of the α-conotoxin. Vc1.1, *Biochem. Pharmacol. 89*, 131-140.
(37) Yu, R., Tae, H.-S., Tabassum, N., Shi, J., Jiang, T., and Adams, D. J. (2018) Molecular determinants conferring the stoichiometric-dependent activity of α-conotoxins at the human α9α10 nicotinic acetylcholine receptor subtype. *J. Med. Chem. 61*, 4628-4634.
(38) Zouridakis, M., Papakyriakou, A., Ivanov, I. A., Kasheverov, I. E., Tsetlin, V., Tzartos, S., and Giastas, P. (2019) Crystal structure of the monomeric extracellular domain of α9 nicotinic receptor subunit in complex with α-conotoxin RgIA: Molecular dynamics insights into RgIA binding to α9α10 nicotinic receptors. *Front. Pharmacol. 10*, 474.
(39) Halai, R., Clark, R. J., Nevin, S. T., Jensen, J. E., Adams, D. J., and Craik, D. J. (2009) Scanning mutagenesis of α-conotoxin Vc1.1 reveals residues crucial for activity at the α9α10 nicotinic acetylcholine receptor. *J. Biol. Chem. 284*, 20275-20284.
(40) Case, D., Cerutti, D., Cheatham III, T., Darden, T., Duke, R., Giese, T., Gohlke, H., Goetz, A., Greene, D., and Homeyer, N. AMBER 2017, 2017, *San Francisco: University of California*.
(41) Maier, J. A., Martinez, C., Kasavajhala, K., Wickstrom, L., Hauser, K. E., and Simmerling, C. (2015) ff14SB: Improving the accuracy of protein side chain and backbone parameters from ff99SB. *J. Chem. Theory & Comput. 11*, 3696-3713.
(42) Dupradeau, F.-Y., Pigache, A., Zaffran, T., Savineau, C., Lelong, R., Grivel, N., Lelong, D., Rosanski, W., and Cieplak, P. (2010) The R.ED. tools: advances in RESP and ESP charge derivation and force field library building. *Physical Chemistry Chemical Physics 12*, 7821-7839.
(43) Olsson, M. H. M., Sondergaard, C. R., Rostkowski, M., and Jensen, J. H. (2011) PROPKA3: Consistent treatment of internal and surface residues in empirical pK(a) predictions. *J. Chem. Theory & Comput. 7*, 525-537.
(44) Miyamoto, S., and Kollman, P. A. (1992) Settle: An analytical version of the SHAKE and RATTLE algorithm for rigid water models. *J. Comput. Chem. 13*, 952–962.
(45) Darden, T., York, D., and Pedersen, L. (1993) Particle mesh Ewald: An N· log (N) method for Ewald sums in large systems. *J. Chem. Phys. 98*, 10089-10092.